analytical chemistry

Article

Cite This: Anal. Chem. 2018, 90, 4422−4428

pubs.acs.org/ac

Soft Picosecond Infrared Laser Extraction of Highly Charged Proteins and Peptides from Bulk Liquid Water for Mass Spectrometry

Yinfei Lu, Cornelius L. Pieterse, Wesley D. Robertson, and R. J. Dwayne Miller*

Max Planck Institute for the Structure and Dynamics of Matter, Luruper Chaussee 149, Hamburg 22761, Germany

Supporting Information

ABSTRACT: We report the soft laser extraction and production of highly charged peptide and protein ions for mass spectrometry directly from bulk liquid water at atmospheric pressure and room temperature, using picosecond infrared laser ablation. Stable ion signal from singly charged small molecules, as well as highly charged biomolecular ions, from aqueous solutions at low laser pulse fluence (~0.3 J cm^{-2}) is demonstrated. Sampling via single picosecond laser pulses is shown to extract less than 27 pL of volume from the sample, producing highly charged peptide and protein ions for mass spectrometry detection. The ablation and ion generation is demonstrated to be soft in nature, producing natively folded proteins ions under sample conditions described for native mass spectrometry. The method provides laser-based sampling flexibility, precision and control with highly charged ion production directly from water at low and near neutral pH. This approach does not require an additional ionization device or high voltage applied directly to the sample.

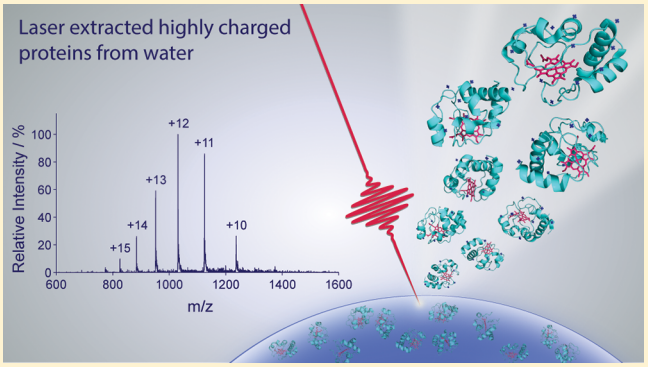

The soft precision controlled extraction of biomolecules from aqueous environments into the gas phase is a crucial step for investigating biological systems. The pioneering methods for large biomolecule gas phase ion production, which include electrospray ionization (ESI),[1] developed following the critical observation of ion production by charged droplet evaporation demonstrated by thermospray,[2] and matrix-assisted laser desorption/ionization (MALDI),[3,4] have facilitated extraordinary biological insight. ESI and subsequent ambient nebulization based methods, have been widely utilized for their ability to softly produce highly charged biomolecules, large proteins and noncovalently bonded complexes for analysis with high stability and sensitivity.[5−15] The highly charged species available has enabled the use of low mass-to-charge ratio (m/z) range mass spectrometers and facilitate fragmentation methods invaluable to proteomic identification.[16]

The control inherent to laser based techniques, such as MALDI, provides sampling flexibility and precision, which is extremely advantageous for high throughput and selective sampling, as well as for mass spectrometry (MS) imaging.[17,18] Conventional MALDI produces primarily singly charged analyte ions and is in general less soft than ESI.[19−21] The matrices employed can introduce undesirable artifacts to MS spectra and adversely affect pre-analysis sample processing for certain scenarios. Innovative solutions utilizing continuous flow liquid MALDI matrix coupled directly to vacuum for laser ionization have been developed to combine analysis with solution separation methods such as liquid chromatography.[22,23] As well, numerous techniques have been developed to enhance analyte charging by combining the laser irradiation of matrix, tissue or aqueous solutions, with a secondary ionization device, with great success.[24−30] Atmospheric pressure (AP) MALDI systems have been utilized to ablate matrix material into the heated transfer capillary of the mass spectrometer where both highly charged peptide and protein ions were produced in the high temperature region.[31,32] The technique has been extended for the direct analysis of solution-analyte mixtures, producing highly charged species without the need for applied voltage, nebulizing gas, volatile solvents or laser irradiation termed "laserspray",[33,34] not to be confused with "laser spray" developed by Hiraoka et al. as described later. Liquid UV-MALDI at a lower laser pulse energy has been demonstrated to provide stable and sensitive (fmol) detection of highly charged ion production from both 2,5-dihydroxybenzoic acid (DHB) and cyano-4-hydroxycinnamic acid (CHCA) matrix mixtures in glycerol and trimethylamine.[35] Highly charged molecular species have also been observed from pulsed nanosecond infrared (IR) irradiation of glycerol matrixes at AP, but with limited sensitivity (50 pmol).[36] The vacuum IR ablation (0.3 to 7.5 J cm^{-2}) of standard matrix as well as water ice has been demonstrated for charged species up to 7+ for select biomolecules.[37−40]

The laser-induced production of highly charged biomolecular ions from liquid water was first demonstrated using IR heating based laser spray, which provided unique advantages over

Received: October 18, 2017
Accepted: March 9, 2018
Published: March 9, 2018

DOI: 10.1021/acs.analchem.7b04306
Anal. Chem. 2018, 90, 4422−4428

ESI.[41−43] The method requires high laser power densities (>5 × 10^4 J cm^{-2} s^{-1}) provided by a continuous wave CO_2 laser (10.6 μm) to initiate thermally and acoustically unconfined ablation. A fast solvent flow is evaporated by the laser, which is focused within a stainless-steel nebulizer held at high voltage, to produce highly charged species similar to ESI.[41−43] The applicability of the method has been somewhat limited due to the rapid sample consumption inherent to the technique. Numerous AP-IR-MALDI (0.3 to 5 J cm^{-2}) studies utilizing pure water solutions, ice or a standard IR-matrix have demonstrated limited charging, producing singly and low charge state biomolecules similar in character to conventional MALDI.[44−48] Similar results have been observed for high-power pulsed irradiation (2.5 J cm^{-2}) using levitated water/methanol (1:1) microdroplets.[49] Additionally, sampling provided by pulsed IR irradiation, from a CO_2 laser (0.3 J cm^{-2}), of pure water-cytochrome *c* solutions held at a high voltage in atmosphere, resulted in spectra similar to ESI, although no other ions were observed from any other samples that were investigated, without ESI postionization.[50] Pulsed IR sampling of a continuous aqueous solution flow interface with post ionization, free of voltage applied directly to the sample, has been demonstrated for nanosecond (5.8 J cm^{-2}) and picosecond (1.9 J cm^{-2}) duration pulses. These methods both required secondary ESI ionization for highly charged ion production, though characterization of direct ionization was not the focus of the work.[27,30]

It is well established that the pulsed IR ablation of water is capable of driving a gas phase ablation plume at several times the speed of sound from the water surface.[51−53] We have shown that this entire process can be conformed to occur faster than both nucleation and cavitation shock wave formation, therefore ensuring the excess energy of the ablation process to be primarily localized in the translational energy of the excited water molecules.[52−54] These conditions are ideal for injecting nominally low vapor pressure water-soluble molecules into the gas phase with the least amount of fragmentation or thermally induced nonlinear processes for mass spectrometry applications. We have utilized picosecond infrared laser (PIRL) ablation, operating under the above-described desorption by impulsive vibrational excitation (DIVE)[52−54] conditions for the soft extraction of biological entities from tissue and water solutions analyzed offline following ablation and collection. The ablation method was shown to extract unmodified proteins and protein complexes with conserved quaternary structure, as well as functionally conserved enzymes, proteins and viruses.[55,56] The PIRL is tuned to 1-photon resonantly excite the vibrational stretching mode of water that relaxes directly to translational motions, driving water, and analyte molecules into the gas phase faster than both the thermal and acoustic relaxation times of the excited volume.[52−54] The physics of the ablation process are equally well adapted for any material removal or laser based biopsy with successful application to numerous clinical surgery scenarios[57−59] and as a cold laser tissue homogenizer to enhance proteome conservation.[60]

Here we apply pulsed picosecond infrared irradiation at low laser energies (40 μJ focused to 0.3 J cm^{-2}) for the soft, stable extraction and production of small molecule ions, as well as highly charged biological molecules, directly from bulk liquid water under atmospheric pressure. Notably, the setup is stable over long times with no secondary ionization device required. The method softly produces highly charged peptide and protein ions, which is typically characteristic for ESI, laser spray and other nebulization based techniques, from pure liquid water over a broad pH range. The laser based method is mechanical contact free, does not require a high speed gas flow or voltage applied directly to the sample, and operates at low sample consumption rates (<27 pL per pulse) with limited energy transfer to the bulk sample. The method provides sampling flexibility for scenarios in which soft, precision online sampling is required.

EXPERIMENTAL METHODS

Experimental Setup. The DIVE-MS system (Figure 1) was constructed by replacing the spray chamber, nebulizer assembly, end plates, insulators and the transfer capillary mounting assembly of an ion trap mass spectrometer (Esquire 3000, Bruker) with a home designed and constructed interface for optimized access to the ablation plume. A long working distance microscope and sample delivery system was implemented to set and control the position of the ablated water/air interface to within 50 μm. Ablation pulses (either single pulse, pulse bursts or continuous 1 kHz operation) were delivered using a diode synchronized fast shutter and synchronized with ion trap collection via a home designed synchronization circuit and software. The sample delivery capillary, sample bead and ablation plume undergoing 1 kHz ablation is shown in Figure S1. A custom designed and constructed transfer capillary extension (Figure 1) was used to divert the heated nitrogen curtain gas (10 L min^{-1}), which also serves as the transfer capillary heating gas, away from the liquid sample and the ablation plume. The modification allowed full temperature and voltage control of the transfer capillary and avoided rapid sample evaporation. Noted in the text when utilized, the plume was also directly collected into the quartz transfer capillary through a standard planar spray shield end plate (Figure S2) held at high voltage. A reduced curtain gas

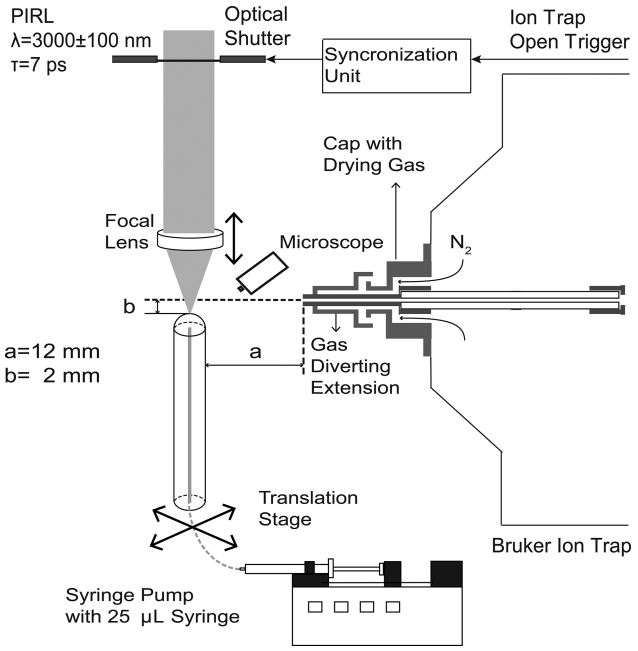

Figure 1. A schematic representation of the sample delivery, ablation, and modified ion trap MS system. Aqueous analyte solutions were delivered via capillary flow and ablated by a PIRL laser, collected and mass-analyzed by a modified ion trap mass spectrometer.

DOI: 10.1021/acs.analchem.7b04306
Anal. Chem. 2018, 90, 4422−4428

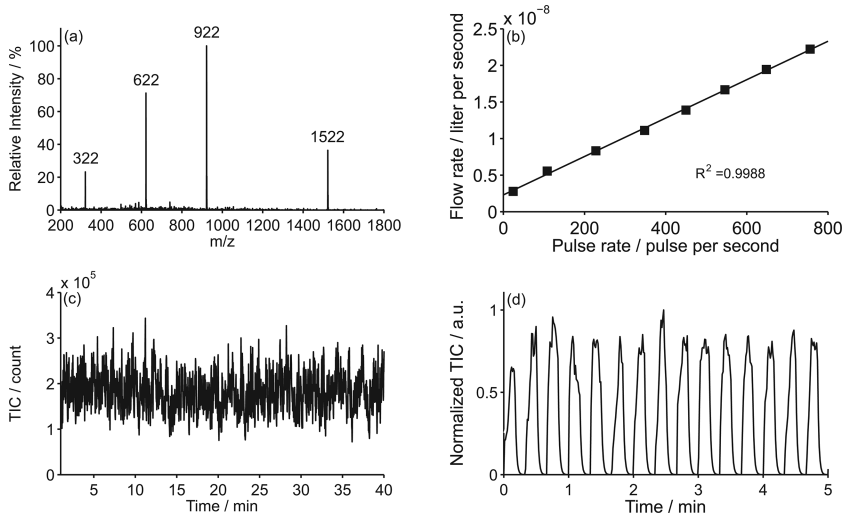

Figure 2. Characterization of PIRL-DIVE ablation of water samples. (a) DIVE-MS spectrum of $[M + H]^+$ of hexamethoxyphosphazene (m/z = 322), hexakis(2,2-difluoroethoxy)phosphazene (m/z = 622), hexakis(1*H*,1*H*,3*H*-tetrafluoropropoxy)phosphazene (m/z = 922), and hexakis(1*H*,1*H*,5*H*-octafluoropentoxy)phosphazene (m/z = 1522) from water containing trifluoroacetic acid ammonium salt (TFA) (93.1 μM) and 5% acetonitrile. The spectrum shown is the average of 5 s of data collection. (b) Sample flow rate versus pulse rate of DIVE ablation of the sample surface. The solid line represents the best fit (R^2 = 0.9988) of the data to a linear curve and resulted in a slope and y-intercept of $m = 26.2 \times 10^{-12}$ and $b = 2.30 \times 10^{-9}$, respectively. (c) Total ion current (TIC) versus time (m/z = 200−2000 range) for the same measurement as in panel a. (d) TIC versus time (m/z = 500−1000 range) during shuttering (20 s) of a 1 kHz ablation pulse train, confirming the DIVE ion signal dependence on laser ablation. Transfer capillary temperature was measured to be 139 °C.

flow (0.5 L min^{-1}) was used with this configuration to minimize sample evaporation and plume disruption. The actual transfer capillary temperature for all experiments was measured directly using a thermocouple. The measured value was lower than the set value when using the significantly reduced gas flow rate as well as with the collection extension. The actual measured transfer capillary temperature is noted in the text for all experiments. Nitrogen was used as the heating gas.

Sample delivery capillary tubing (precut natural PEEK, 1/16 in. outer diameter, and 0.030-in. inner diameter, TPK130, VICI) was connected to a syringe (Hamilton, 25 μL) and a syringe pump (KD Scientific) to set the sample flow rate. The exit of the PEEK sample capillary was cleaved and mounted with custom holders and mounts with the flat face of the sample capillary vertical and in front of the transfer capillary extension, or planar end plate, of the MS interface for sample ablation. The exit of the sample capillary was aligned 22 mm below the position of focal point of the laser beam. The PIRL laser was directed downward toward the sample capillary with the focal position located 12 mm away from the collection entrance and 2 mm directly below the MS ion transfer capillary axis. For each experiment, 25 μL of analyte solution was loaded into the sample syringe. A volume (<5 μL) was flushed through the PEEK tubing to produce a stable bead of aqueous sample solution (~1.9 μL), stabilized and maintained by optimizing the solution flow rate and ablation frequency. This resulted in the total amount of analyte loaded into the 25 μL syringe ranging between 250 fmol and 250 pmol, for 10 nM and 10 μM solutions, respectively. A digital long working distance microscope (Dino-lite, AD7013MTL (R4)) was used to image the sample bead. The resulting sample meniscus and laser ablation plume images provided feedback for system alignment and signal optimization. The syringe and peek sample tubing were flushed with acetone, isopropanol, and water (1 mL each), 3 cycles, between samples. This could be accomplished in roughly 1 min. No sample contamination was observed.

DIVE-MS and ESI were performed under the optimized conditions for each method and the particular molecular species. The transfer capillary voltage of the ion trap MS was set to ±4500 V (negative and positive ion modes respectively), with a spray shield end plate offset of 500 V for both methods. Mass spectra were acquired using ESI, as the control, by mounting and optimizing the ESI nebulizer position at a right angle to the MS collection interface. Samples were delivered via a standard electrospray nebulizer (electrically grounded) with a helium nebulizer gas curtain (10 psi) and heated nitrogen curtain drying gas (10 L min^{-1}). All data were collected and analyzed using Bruker Daltonics Data Analysis software. The spectra displayed for both DIVE-MS and ESI-MS are the results of averaging 1 min of sample collection, unless when otherwise noted. The ion trap accumulation time was set to 50 ms. Collision induced dissociation measurements were performed with the precursor ion mass isolation window set to 4 mass units (m/z of the precursor ion ±2) and the fragmentation time to 40 ms. Helium was used as the collision gas and the fragmentation amplitude was varied to achieve the required degree of fragmentation. Throughout, ablation pulse bursts produced by a synchronized shutter operating at 6 Hz, containing 4 pulse bursts, and a sample flow rate of 167 nL min^{-1}, were found to be optimal and were thus employed, unless when otherwise noted.

Laser System. A PIRL, model PIRL-APLQ-3000 from Attodyne Inc., Canada, was used to deliver irradiation at the wavelength of 3000 ± 100 nm, with a pulse duration of 7 ps at a repetition rate of 1 kHz. A home-built optical system was used for beam delivery and equipped with a fast, diode synchronized high-speed external shutter for control of single and burst mode pulse selection with home designed LabVIEW software. The PIRL beam was focused onto the sample with a 25 mm calcium fluoride lens resulting in a transverse beam diameter ($1/e^2$) at

DOI: 10.1021/acs.analchem.7b04306
Anal. Chem. 2018, 90, 4422−4428

the focus of approximately 140 μm as measured by a WinCamD-FIR2−16-HRR camera. The DIVE ablation pulse energy was measured at the focal plane to be 40 μJ per pulse. The lens was adjusted to optimize ion production and ablation stability.

Sample Preparation. Stock samples and solutions of caffeine (≥99%, HPLC, MW 194.19), angiotensin I acetate salt hydrate (≥90%, HPLC, MW 1296.48), angiotensin II human (≥93%, HPLC, MW 1046.18), cytochrome *c* from equine heart (≥95%, SDS-PAGE, MW 12,384), lysozyme from chicken egg white (≥90%, single chain MW 14,300), acetic acid (≥99.99%), formic acid (LC-MS Ultra), and ammonium acetate (≥99%, HPLC), ammonium bicarbonate (≥99.5%, BioUltra), were purchased from Sigma-Aldrich Chemie GmbH (Munich, Germany). Deionized distilled water from a PURELAB Classics (>18.5 MΩ cm, ELGA) system was used. Ion trap ESI tuning mix (G2431a) was purchased from Agilent Deutschland GmbH (Waldbronn, Germany). All analytes, including peptides and proteins, were used without further purification.

All DIVE-MS solutions were prepared in pure deionized distilled water with or without acetic acid or formic acid (0.1−1%, v/v) as noted in the text. Native protein solutions were prepared on ice and in 10−50 mM ammonium acetate or ammonium bicarbonate buffer with the pH (7.0) adjusted as described previously.[10] ESI tuning mix was added to pure water at a ratio of 1:20 (v/v), resulting in a final solution containing; hexamethoxyphosphazene (71 nM, MW 321.14), hexakis (2,2-difluoroethoxy)phosphazene (357 nM, MW 621.19), hexakis (1H, 1H, 3H-tetrafluoropropoxy)phosphazene (986 nM, MW 921.19), hexakis (1H, 1H, 5H-octafluoropentoxy)phosphazene (949 nM, MW 1521.33) with trifluoroacetic acid ammonium salt (TFA) (93 μM) and 5% acetonitrile. ESI samples were prepared from the same stock solutions to the same analyte and acid concentration as the DIVE-MS samples.

RESULTS AND DISCUSSION

PIRL ablation was stabilized at the water/air interface by means of adjusting the sample surface via feedback from the long-working-distance microscope and by adjustments to the sample delivery and laser control system. The PIRL ablation rate for MS analysis was performed in burst mode at 6 Hz, 4 pulses per burst, unless otherwise noted. The DIVE-MS setup was characterized and optimized by using the phosphazene variants from ESI tuning mix dissolved in pure water. As shown in Figure 2a, direct ablation of the sample resulted in a spectrum composed of singly charged species, $[M + H]^+$, of hexamethoxyphosphazene (m/z = 322), hexakis(2,2-difluoroethoxy)phosphazene (m/z = 622), hexakis(1*H*,1*H*,3*H*-tetrafluoropropoxy)phosphazene (m/z = 922), and also hexakis(1*H*,1*H*,5*H*-octafluoropropoxy)phosphazene (m/z = 1522). The flow rate required to maintain the sample interface (±50 μm relative to the laser focal plane) over a range of pulse rates was measured and used to estimate the ablated volume of the liquid per laser pulse (Figure 2b). Ablation was performed at 6 Hz with the pulse number ranging from 4 to 126 pulses per burst (24−756 pulses per second). The resulting slope of the fitting curve indicated the extracted volume from the bulk water, per laser pulse, was less than 27 pL. This value corresponds to an effective DIVE extraction depth of ∼1.5 μm per pulse of the water surface, within the range predicted by fluid dynamics models.[50] Considering the analyte concentration and extraction volume, the hexamethoxyphosphazene ion, as shown in Figure 2a, is the result of the consumption of 223 amol analyte when averaging for 5 s. For the same sample, the spectrum following 1 s of signal averaging (24 ablation events) is still easily discernible (Figure S3), corresponding to 48 amol of analyte consumption. As shown in Figure 2c, the total ion current (TIC) was within 1 order of magnitude of that achieved with standard ESI (>10^5 counts). The closing of the laser shutter (20 s intervals) was implemented to segment 1 kHz pulse trains to confirm the ablation dependence of the MS signal. As shown in Figure 2d, the TIC decreased to baseline values following the shutter closing.

DIVE-MS was also applied to aqueous solutions of small molecule drugs and compared to standard ESI (Figure S4). Acetaminophen dissolved in water containing 0.5% formic acid (v/v) resulted in the characteristic protonated species, $[M + H]^+$ (m/z = 152), with no additional thermal or hydrolytic degradation fragment peaks, for which it is known to be susceptible.[61] Additionally, the singly charged species of acetaminophen were produced from pure water solutions (no acid added), with 10 nM solutions being successfully analyzed, corresponding to a total consumption of 39 amol of analyte (Figure S5). Caffeine dissolved in water containing 0.1% acetic acid (v/v) displayed characteristic protonated species $[M + H]^+$ (m/z = 195) as well, without additional fragmentation (Figure S4). Approximately an order of magnitude reduction in sample consumption was possible with DIVE-MS, as compared to standard ESI on the same modified mass spectrometer.

To evaluate the capabilities of DIVE-MS for highly charged ion production, the peptide angiotensin I (10 μM), in a water solution containing 0.1% formic acid, was analyzed (Figure 3a).

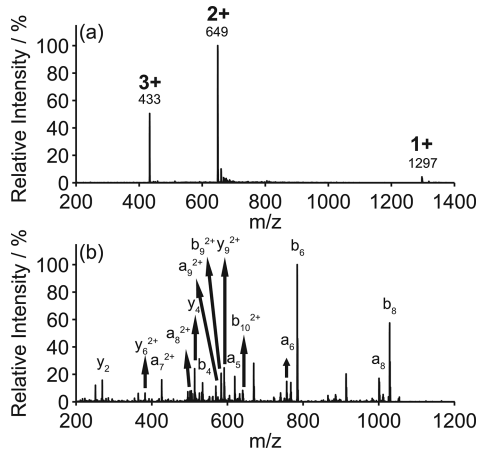

Figure 3. (a) DIVE-MS mass spectrum displaying the $[M + H]^+$, $[M + 2H]^{2+}$, and the $[M + 3H]^{3+}$ species of the peptide angiotensin I. The sample was 10 μM in water contained 0.1% formic acid (v/v). (b) DIVE-MS/MS CID spectrum of the doubly charged species, $[M + 2H]^{2+}$, of angiotensin I. Transfer capillary temperature was measured to be 199 °C.

The charged species observed following PIRL ablation of the aqueous peptide sample were similar in form to spectra generated by ESI (Figure S6a). The spectrum of angiotensin I indicated the $[M + H]^+$, $[M+2H]^{2+}$, and $[M+3H]^{3+}$ species at m/z = 1297, 649, and 433 respectively, with observable fractions (<10%) of adduct ions produced. The signal-to-noise obtained was comparable to that produced using standard ESI with the modified setup. For the spectrum shown, an order of magnitude decrease in the sample consumption rate was used as compared to ESI, 167 nL min^{-1} versus 3 μL min^{-1}, similar to

DOI: 10.1021/acs.analchem.7b04306
Anal. Chem. 2018, 90, 4422−4428

nanospray. The rate is adjustable and dependent on the laser sampling frequency as shown in Figure 2b. The TIC produced from the peptide solution was stable (Figure S7) and comparable in intensity to that of standard ESI, which facilitated the generation of DIVE-MS/MS spectra using fragmentation by collisionally induced dissociation (CID). The MS/MS CID spectrum of the $[M + 2H]^{2+}$ species of angiotensin I produced by DIVE-MS is shown in Figure 3b, with the corresponding ESI-MS and ESI-MS/MS spectra shown in Figure S6b. The MS/MS spectra generated by these two methods were nearly identical, demonstrating the stable production of highly charged ions for tandem mass spectrometry, as is typically utilized by standard nebulization based methods for fragmentation based proteomic identification. Successful MS analysis was as well performed from 10 nM aqueous solutions (with 0.1% formic acid) of both angiotensin I and angiotensin II with a transfer capillary temperature of 139 °C (Figure S5). The doubly charged species $[M + 2H]^{2+}$ was detected for the consumption of amounts as low as 39 amols analyte.

Charged species production and detection from single PIRL laser pulses (27 pL extraction) was implemented using angiotensin I (10 μM) in pure water (Figure S8). Modifications were made to the laser control and trap synchronization system to allow a single laser pulse to sample the solution and MS analysis performed on the single ablation plume event. The spectrum exhibited the singly, doubly and triply charge states of the peptide, with reproducible signal over long measurement times (Figure S9). The potential for single shot sampling and analysis with highly charged species production makes the technique particularly interesting for a high-throughput lab-on-a-chip coupling for proteomic investigation.

Highly charged protein ions extracted from bulk water solutions with PIRL were observed. As shown in Figure 4a, cytochrome *c* (10 μM) in water containing 0.1% formic acid resulted in a distribution of highly charged positive protein ions centered at 12+, consistent with the unfolded form of the protein observed in ESI studies.[62] The measurement was performed at a measured transfer capillary temperature of 74 °C using the heated collection extension. The charge state distribution of the cytochrome *c* ions was observed to be dependent on the sample and collection conditions, as previously reported.[63,64] A broad charge distribution centered at 8+ was observed for cytochrome *c* water solutions with the addition of 0.5% acetic acid (Figure S10a). The transfer capillary temperature was 36 °C and the data collected without the transfer extension. Highly negatively charged cytochrome *c* ions were observed from the same acidic solution (Figure S10b), without the addition of a base, in negative-ion mode operation. Similar results have been observed using standard laser spray, where IR ablation of water is performed within a nebulizer, and the ability to observe negative ions attributed to field induced species enrichment near the sample surface by the applied electric field.[42,65]

Pure water solutions containing cytochrome *c* (10 μM), without the addition of acid, were also investigated (Figure 4b), resulting in highly charged species production. A slight shift in the charge state distribution, from 12+ to 11+, was observed without the addition of acid, as well as an increase in the adduct abundance (Figure S11), a reflection of the population increase of the species in the near neutral pH sample. A decrease in the TIC was noted for the pure water sample though the spectra are easily discernible for the 374 fmol of analyte consumed. The

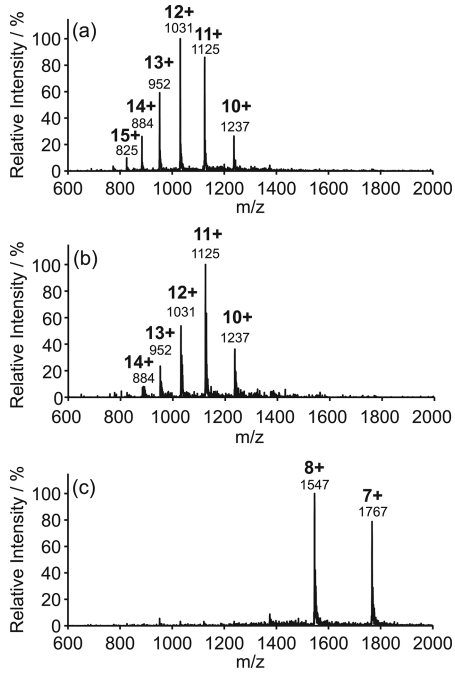

Figure 4. DIVE-MS spectrum of (10 μM) cytochrome *c* (a) in water containing 0.1% formic acid, (b) in acid-free pure water, and (c) in 10 mM ammonium acetate buffer. Transfer capillary temperature was measured to be 74 °C for panels a and b. For panel c, no gas diverting heated transfer extension was applied and the transfer capillary temperature was measured to be 62 °C.

increase in ion signal at low pH is likely due to the higher concentration of protons in solution available for protonation as well the increase has been proposed to contribute to charged droplets formation in ESI type processes. Pure water solutions without the addition of acid, for angiotensin I and II, and also acetaminophen, showed the same charging states (Figure S12) (transfer capillary temperature 139 °C) as compared to samples prepared at lower pH by the addition of acid. A decrease was observed in the 3+ state for angiotensin I in pure water as well as an increase in adduct formation. This is assumed to be due to the decrease concentration of protons in solution available for analyte protonation.

DIVE-MS was further applied to protein solutions prepared under sample conditions described for native MS, without the use of the additional gas diverting heated transfer extension and with a measured transfer capillary temperature of 62 °C.[9] Cytochrome c samples resulted in a spectrum (Figure 4c) composed of the +7 and +8 charge state species. The narrow distribution indicated the detected species of the protein to be in the folded native state, being softly extracted from the sample solution. The spectrum is comparable with that produced by means of standard ESI and is an indication of the soft nature of the ablation method.[62] Highly charged species were observed as well from the protein lysozyme (Figure S13). The spectrum indicated a mixture of the folded and unfolding state, likely due to the sampling conditions employed.

During DIVE ablation, water and analyte molecules within a thin layer of the liquid/air interface are driven into the gas phase at supersonic velocity, stripping analytes of bound water molecules.[51,53] Recently, molecular dynamics simulations, which characterized DIVE ablation for a protein counterion system in water, have shown that the mechanism is capable of achieving direct desolvation for gas phase ion production in

DOI: 10.1021/acs.analchem.7b04306
Anal. Chem. 2018, 90, 4422−4428

vacuum with minimal analyte damage.[66] Under the ambient conditions described here, atmospheric collision of the supersonic plume likely leads to cooling and droplet formation of the gas phase ablation plume. It is also possible that ion signal could originate from charged droplets directly ejected from the ablation site with subvaporization enthalpy,[53] similarly as produced initially in methods such as ESI and laser spray or by electrostatic charging following laser disruption of the liquid surface.[67] A transfer capillary temperature dependence revealed no change in the charge state distribution of cytochrome *c* (Figures S14 and S15) as a function of temperature but an increase in the TIC indicated some fraction of proteins were not completely desolvated as they entered the MS, similar as observed for ESI under lower than optimized desolvation conditions. This is likely due to the initial incomplete shedding of water molecules bound to the protein in the gas phase ablation plume, subsequent condensation of the gas phase water vapor/analyte in the atmosphere or incomplete evaporation of charged droplets.

It should be noted that experiments performed using the heated extension are free of curtain gas to assist in desolvation and experiments performed without the extension only utilized a minimal curtain gas flow (0.5 L min^{-1}). The ion signal was observed to be dependent on the voltage applied to the collection extension and transfer capillary, as shown for cytochrome *c* in Figure S16. Minimal MS signal was observed for voltages from 0 to −1500 V. The signal increased sharply from −1500 to −3500 V. The measurement does not however differentiate voltage dependent effects on the sample, those effecting charging or collection efficiency, from voltage dependent ion production effects that may occur inside the transfer capillary.

To investigate in the region in which charged species are produced by DIVE ablation, an electrically isolated, conductive planar mesh grid was placed between the liquid sample and the collection extension. The voltage applied to the grid was varied while the voltage of the quartz transfer capillary remained constant (−4500 V). No ion signal was observed without a voltage applied to the grid. A positive ion signal steadily increased with increased negative voltage applied to the grid, as shown in Figure S17, indicating the presence of charged species or droplets outside the MS transfer capillary. Enhanced charging by field-induced separation of ions within a bulk liquid sample has been proposed to contribute to the ionization mechanism and sensitivity observed by traditional laser spray, as well attributed to the large negative ion signals observed.[41] The large required electric field (~6×10^4 V cm^{-1}) for laser spray has been attributed to producing an ion mobility high enough to overcome the high linear velocity of the solution within the high flow sample nebulizer (~3 cm s^{-1}).[41] However, for DIVE-MS, the linear velocity of the sample flow is substantially lower (6×10^{-5} cm s^{-1}) due to the ability to operate at low sample consumption rates. Therefore, charged analytes within the sample would have sufficient velocity even at lower field values, for separation and localization near the surface. The result indicates the mechanism may contribute to enhanced ion production. Subsequent studies will further characterize the mechanism for obtaining the highly charged ion species with the noted sensitivity.

CONCLUSIONS

We demonstrate a soft mass spectrometry interface which couples the picosecond infrared laser sample extraction directly to an ion trap mass spectrometer inlet without requiring a post-ionization device or high voltage applied directly to the sample solution. Ion signals from highly charged biomolecular ion species, as well singly charged small molecules, are produced by this method, which drives ablation on time scales under thermal and acoustic stress confinement for efficient coupling to translational motions and reduction of fragmentation. In addition, native protein mass spectra are obtained by employing native buffer solution. It is postulated that ionization occurs as a result of the direct desolvation of analytes from the solution or the subsequent formation of charged droplets via the cooling of the ablation plume in atmosphere. Further experiments are required to investigate the underlying ionization mechanism. In addition, it is shown that single laser pulses can be employed to extract 27 pL sample volumes. The low sample consumption, combined with the capability to produce highly charged ions, makes the method interesting for coupling to liquid chromatography or microfluidic lab-on-a-chip devices.

ASSOCIATED CONTENT

Supporting Information

Additional information as noted in the text. The Supporting Information is available free of charge on the ACS Publications Web site. The Supporting Information is available free of charge on the ACS Publications website at DOI: 10.1021/acs.analchem.7b04306.

(PDF)

AUTHOR INFORMATION

Corresponding Author

*E-mail: dwayne.miller@mpsd.mpg.de.

ORCID

Wesley D. Robertson: 0000-0001-9526-4217

R. J. Dwayne Miller: 0000-0003-0884-0541

Author Contributions

Y.L. and W.D.R. contributed equally. The manuscript was written through contributions of all authors. All authors have given approval to the final version of the manuscript.

Notes

The authors declare the following competing financial interest(s): R. J. Dwayne Miller is the author of a patent related to the mechanism of PIRL laser ablation.

ACKNOWLEDGMENTS

We would like to thank Djordje Gitaric and Josef Gonschior for their valuable design and engineering contributions, as well as Erik Friedling for designing the capillary extension. We would also like to thank Jean-Michel Boudreau for his efforts in native buffer preparation and Maria Grigera for her graphical contributions. This work was supported by the Max Planck Institute.

REFERENCES

(1) Yamashita, M.; Fenn, J. B. *J. Phys. Chem.* **1984**, *88*, 4451−4459.

(2) Blakley, C. R.; McAdams, M. J.; Vestal, M. L. *J. Chromatogr. A* **1978**, *158*, 261−276.

(3) Karas, M.; Hillenkamp, F. *Anal. Chem.* **1988**, *60*, 2299−2301.

(4) Tanaka, K.; Waki, H.; Ido, Y.; Akita, S.; Yoshida, Y.; Yoshida, T.; Matsuo, T. *Rapid Commun. Mass Spectrom.* **1988**, *2*, 151−153.

(5) Fenn, J. B.; Mann, M.; Meng, C. K.; Wong, S. F.; Whitehouse, C. M. *Science* **1989**, *246*, 64−71.

(6) Wilm, M.; Mann, M. *Anal. Chem.* **1996**, *68*, 1−8.

DOI: 10.1021/acs.analchem.7b04306
Anal. Chem. 2018, 90, 4422−4428

(7) Wilm, M. S.; Mann, M. *Int. J. Mass Spectrom. Ion Processes* **1994**, *136*, 167−180.
(8) Hirabayashi, A.; Sakairi, M.; Koizumi, H. *Anal. Chem.* **1994**, *66*, 4557−4559.
(9) Takáts, Z.; Wiseman, J. M.; Gologan, B.; Cooks, R. G. *Anal. Chem.* **2004**, *76*, 4050−4058.
(10) Jecklin, M. C.; Touboul, D.; Bovet, C.; Wortmann, A.; Zenobi, R. *J. Am. Soc. Mass Spectrom.* **2008**, *19*, 332−343.
(11) Harris, G. A.; Galhena, A. S.; Fernández, F. M. *Anal. Chem.* **2011**, *83*, 4508−4538.
(12) Alberici, R. M.; Simas, R. C.; Sanvido, G. B.; Romão, W.; Lalli, P. M.; Benassi, M.; Cunha, I. B. S.; Eberlin, M. N. *Anal. Bioanal. Chem.* **2010**, *398*, 265−294.
(13) Takáts, Z.; Wiseman, J. M.; Gologan, B.; Cooks, R. G. *Science* **2004**, *306*, 471−473.
(14) Heron, S. R.; Wilson, R.; Shaffer, S. A.; Goodlett, D. R.; Cooper, J. M. *Anal. Chem.* **2010**, *82*, 3985−3989.
(15) Cody, R. B.; Laramée, J. A.; Durst, H. D. *Anal. Chem.* **2005**, *77*, 2297−2302.
(16) Han, X.; Aslanian, A.; Yates, J. R., III *Curr. Opin. Chem. Biol.* **2008**, *12*, 483−490.
(17) Lee, J.; Soper, S. A.; Murray, K. K. *Anal. Chim. Acta* **2009**, *649*, 180−190.
(18) Caprioli, R. M.; Farmer, T. B.; Gile, J. *Anal. Chem.* **1997**, *69*, 4751−4760.
(19) Schulz, E.; Karas, M.; Rosu, F.; Gabelica, V. *J. Am. Soc. Mass Spectrom.* **2006**, *17*, 1005−1013.
(20) Covey, T. R.; Schneider, B. B.; Javaheri, H.; LeBlanc, J. C. Y.; Ivosev, G.; Corr, J. J.; Kovarik, P. In *Electrospray and MALDI Mass Spectrometry*; Cole, R. B., Ed.; John Wiley & Sons, Inc.: Hoboken, NJ, USA, 2010; pp 441−490.
(21) Dreisewerd, K. *Chem. Rev.* **2003**, *103*, 395−426.
(22) Li, L.; Wang, A. P. L.; Coulson, L. D. *Anal. Chem.* **1993**, *65*, 493−495.
(23) Murray, K. K.; Russell, D. H. *Anal. Chem.* **1993**, *65*, 2534−2537.
(24) Sampson, J. S.; Hawkridge, A. M.; Muddiman, D. C. *J. Am. Soc. Mass Spectrom.* **2006**, *17*, 1712−1716.
(25) Nemes, P.; Vertes, A. *Anal. Chem.* **2007**, *79*, 8098−8106.
(26) Rezenom, Y. H.; Dong, J.; Murray, K. K. *Analyst* **2008**, *133*, 226−232.
(27) Huang, F.; Murray, K. K. *Rapid Commun. Mass Spectrom.* **2010**, *24*, 2799−2804.
(28) Robichaud, G.; Barry, J. A.; Muddiman, D. C. *J. Am. Soc. Mass Spectrom.* **2014**, *25*, 319−328.
(29) Flanigan, P.; Levis, R. *Annu. Rev. Anal. Chem.* **2014**, *7*, 229−256.
(30) Zou, J.; Talbot, F.; Tata, A.; Ermini, L.; Franjic, K.; Ventura, M.; Zheng, J.; Ginsberg, H.; Post, M.; Ifa, D. R.; Jaffray, D.; Miller, R. J. D.; Zarrine-Afsar, A. *Anal. Chem.* **2015**, *87*, 12071−12079.
(31) Trimpin, S.; Inutan, E. D.; Herath, T. N.; McEwen, C. N. *Mol. Cell. Proteomics* **2010**, *9*, 362−367.
(32) Trimpin, S.; Inutan, E. D.; Herath, T. N.; McEwen, C. N. *Anal. Chem.* **2010**, *82*, 11−15.
(33) Pagnotti, V. S.; Inutan, E. D.; Marshall, D. D.; McEwen, C. N.; Trimpin, S. *Anal. Chem.* **2011**, *83*, 7591−7594.
(34) Trimpin, S.; Wang, B.; Inutan, E. D.; Li, J.; Lietz, C. B.; Harron, A.; Pagnotti, V. S.; Sardelis, D.; McEwen, C. N. *J. Am. Soc. Mass Spectrom.* **2012**, *23*, 1644−1660.
(35) Cramer, R.; Pirkl, A.; Hillenkamp, F.; Dreisewerd, K. *Angew. Chem., Int. Ed.* **2013**, *52*, 2364−2367.
(36) König, S.; Kollas, O.; Dreisewerd, K. *Anal. Chem.* **2007**, *79*, 5484−5488.
(37) Overberg, A.; Karas, M.; Bahr, U.; Kaufmann, R.; Hillenkamp, F. *Rapid Commun. Mass Spectrom.* **1990**, *4*, 293−296.
(38) Berkenkamp, S.; Karas, M.; Hillenkamp, F. *Proc. Natl. Acad. Sci. U. S. A.* **1996**, *93*, 7003−7007.
(39) Pirkl, A.; Soltwisch, J.; Draude, F.; Dreisewerd, K. *Anal. Chem.* **2012**, *84*, 5669−5676.
(40) Witt, L.; Pirkl, A.; Draude, F.; Peter-Katalinić, J.; Dreisewerd, K.; Mormann, M. *Anal. Chem.* **2014**, *86*, 6439−6446.
(41) Hiraoka, K.; Saito, S.; Katsuragawa, J.; Kudaka, I. *Rapid Commun. Mass Spectrom.* **1998**, *12*, 1170−1174.
(42) Kudaka, I.; Kojima, T.; Saito, S.; Hiraoka, K. *Rapid Commun. Mass Spectrom.* **2000**, *14*, 1558−1562.
(43) Hiraoka, K. *J. Mass Spectrom.* **2004**, *39*, 341−350.
(44) Laiko, V. V.; Taranenko, N. I.; Berkout, V. D.; Yakshin, M. A.; Prasad, C. R.; Lee, H. S.; Doroshenko, V. M. *J. Am. Soc. Mass Spectrom.* **2002**, *13*, 354−361.
(45) Von Seggern, C. E.; Moyer, S. C.; Cotter, R. J. *Anal. Chem.* **2003**, *75*, 3212−3218.
(46) Hiraguchi, R.; Hazama, H.; Masuda, K.; Awazu, K. *J. Mass Spectrom.* **2015**, *50*, 65−70.
(47) Coon, J. J.; Harrison, W. W. *Anal. Chem.* **2002**, *74*, 5600−5605.
(48) Von Seggern, C. E.; Gardner, B. D.; Cotter, R. J. *Anal. Chem.* **2004**, *76*, 5887−5893.
(49) Warschat, C.; Stindt, A.; Panne, U.; Riedel, J. *Anal. Chem.* **2015**, *87*, 8323−8327.
(50) Sampson, J. S.; Muddiman, D. C. *Rapid Commun. Mass Spectrom.* **2009**, *23*, 1989−1992.
(51) Vogel, A.; Venugopalan, V. *Chem. Rev.* **2003**, *103*, 577−644.
(52) Franjic, K.; Cowan, M. L.; Kraemer, D.; Miller, R. J. D. *Opt. Express* **2009**, *17*, 22937−22959.
(53) Franjic, K.; Miller, R. J. D. *Phys. Chem. Chem. Phys.* **2010**, *12*, 5225−5239.
(54) Siwick, B. J.; Dwyer, J. R.; Jordan, R. E.; Miller, R. J. D. *Science* **2003**, *302*, 1382−1385.
(55) Kwiatkowski, M.; Wurlitzer, M.; Omidi, M.; Ren, L.; Kruber, S.; Nimer, R.; Robertson, W. D.; Horst, A.; Miller, R.; Schlüter, H. *Angew. Chem., Int. Ed.* **2015**, *54*, 285−288.
(56) Ren, L.; Robertson, W. D.; Reimer, R.; Heinze, C.; Schneider, C.; Eggert, D.; Truschow, P.; Hansen, N.-O.; Kroetz, P.; Zou, J.; Miller, R. J. D. *Nanotechnology* **2015**, *26*, 284001.
(57) Amini-Nik, S.; Kraemer, D.; Cowan, M. L.; Gunaratne, K.; Nadesan, P.; Alman, B. A.; Miller, R. J. D. *PLoS One* **2010**, *5*, e13053.
(58) Böttcher, A.; Kucher, S.; Knecht, R.; Jowett, N.; Krötz, P.; Reimer, R.; Schumacher, U.; Anders, S.; Münscher, A.; Dalchow, C.; Miller, R. J. D. *Eur. Arch. Otorhinolaryngol.* **2015**, *272*, 941−948.
(59) Jowett, N.; Wöllmer, W.; Reimer, R.; Zustin, J.; Schumacher, U.; Wiseman, P. W.; Mlynarek, A. M.; Böttcher, A.; Dalchow, C. V.; Lörincz, B. B.; Knecht, R.; Miller, R. J. D. *Otolaryngol.–Head Neck Surg.* **2014**, *150*, 385−393.
(60) Kwiatkowski, M.; Wurlitzer, M.; Krutilin, A.; Kiani, P.; Nimer, R.; Omidi, M.; Mannaa, A.; Bussmann, T.; Bartkowiak, K.; Kruber, S.; Uschold, S.; Steffen, P.; Lübberstedt, J.; Küpker, N.; Petersen, H.; Knecht, R.; Hansen, N. O.; Zarrine-Afsar, A.; Robertson, W. D.; Miller, R. J. D.; Schlüter, H. *J. Proteomics* **2016**, *134*, 193−202.
(61) Gilpin, R. K.; Zhou, W. *J. Chromatogr. Sci.* **2004**, *42*, 15−20.
(62) Konermann, L.; Douglas, D. J. *J. Am. Soc. Mass Spectrom.* **1998**, *9*, 1248−1254.
(63) Shi, X.; Takamizawa, A.; Nishimura, Y.; Hiraoka, K.; Akashi, S. *Rapid Commun. Mass Spectrom.* **2008**, *22*, 1430−1436.
(64) Šamalikova, M.; Matečko, I.; Müller, N.; Grandori, R. *Anal. Bioanal. Chem.* **2004**, *378*, 1112−1123.
(65) Hiraoka, K.; Asakawa, Y.; Yamamoto, Y.; Nakamura, M.; Ueda, K. *Rapid Commun. Mass Spectrom.* **2001**, *15*, 2020−2026.
(66) Zou, J.; Wu, C.; Robertson, W. D.; Zhigilei, L. V.; Miller, R. J. D. *J. Chem. Phys.* **2016**, *145*, 204202.
(67) Qiao, L.; Sartor, R.; Gasilova, N.; Lu, Y.; Tobolkina, E.; Liu, B.; Girault, H. H. *Anal. Chem.* **2012**, *84*, 7422−7430.

DOI: 10.1021/acs.analchem.7b04306
Anal. Chem. 2018, 90, 4422−4428